Constitutive activated Cdc42-associated kinase (Ack) phosphorylation at arrested endocytic clathrin-coated pits of cells that lack dynamin

Hongying Shen[a], Shawn M. Ferguson[a], Noah Dephoure[b], Ryan Park[a], Yan Yang[c], Laura Volpicelli-Daley[a], Steven Gygi[b], Joseph Schlessinger[c], and Pietro De Camilli[a]

[a]Department of Cell Biology, Howard Hughes Medical Institute, Program in Cellular Neuroscience, Neurodegeneration and Repair, and Kavli Institute for Neuroscience, Yale University School of Medicine, New Haven, CT 06510; [b]Department of Cell Biology, Harvard University Medical School, Boston, MA 02115; [c]Department of Pharmacology, Yale University School of Medicine, New Haven, CT 06510

ABSTRACT **Clathrin-mediated endocytosis is a fundamental cellular process conserved from yeast to mammals and is an important endocytic route for the internalization of many specific cargos, including activated growth factor receptors. Here we examined changes in tyrosine phosphorylation, a representative output of growth factor receptor signaling, in cells in which endocytic clathrin-coated pits are frozen at a deeply invaginated state, that is, cells that lack dynamin (fibroblasts from dynamin 1, dynamin 2 double conditional knockout mice). The major change observed in these cells relative to wild-type cells was an increase in the phosphorylation state, and thus activation, of activated Cdc42-associated kinase (Ack), a nonreceptor tyrosine kinase. Ack is concentrated at clathrin-coated pits, and binds clathrin heavy chain via two clathrin boxes. RNA interference–based approaches and pharmacological manipulations further demonstrated that the phosphorylation of Ack requires both clathrin assembly into endocytic clathrin-coated pits and active Cdc42. These findings reveal a link between progression of clathrin-coated pits to endocytic vesicles and an activation–deactivation cycle of Ack.**

Monitoring Editor
David G. Drubin
University of California, Berkeley

Received: Jul 27, 2010
Revised: Nov 12, 2010
Accepted: Dec 9, 2010

INTRODUCTION

Clathrin-mediated endocytosis is a form of endocytosis that cells use for the selective internalization of surface molecules and of extracellular material. One of its key functions is to internalize activated growth factor receptors with an important impact on their cellular signaling and degradation. Depending on a variety of factors, internalization represents a mechanism to terminate growth factor receptor signaling or to fully activate, propagate, or modify their cellular responses (Ceresa and Schmid, 2000; Di Fiore and De Camilli, 2001; Miaczynska *et al.*, 2004; Sorkin and von Zastrow, 2009; Lemmon and Schlessinger, 2010).

A variety of approaches have been used to gain insight into the role of endocytosis on growth factor receptor signaling, including silencing RNA methods to suppress expression of clathrin and other endocytic factors, as well as dominant negative interference approaches. The results of these experiments, however, can be affected by incomplete knockdowns, potential scaffolding properties of the clathrin coats, and the effects of dominant negative mutant proteins on their interacting partners. An alternative approach is the use of cells in which genes have been inactivated or "knocked out" by homologous recombination. We recently generated fibroblast cell lines from dynamin 1, dynamin 2 double conditional knockout mice expressing tamoxifen-inducible Cre recombinase (Ferguson *et al.*, 2009). These cells lose dynamin expression upon treatment with 4-hydroxytamoxifen (referred to henceforth as DKO cells). Following dynamin depletion, clathrin-mediated endocytosis is potently

This article was published online ahead of print in MBoC in Press (http://www.molbiolcell.org/cgi/doi/10.1091/mbc.E10-07-0637) on December 17, 2010.

Address correspondence to: Pietro De Camilli (pietro.decamilli@yale.edu).

Abbreviations used: Ack, activated Cdc42-associated kinase; CHC, clathrin heavy chain; CLC, clathrin light chain; CRIB domain, a Cdc42/Rac interactive binding domain; DKO cells, dynamin 1, dynamin 2 double conditional knockout cells; EGFR, epidermal growth factor receptor; GEF, guanine-nucleotide exchange factor; GFP, green fluorescent protein; GST, glutathione *S*-transferase; RFP, red fluorescent protein; RNAi, RNA interference; SAM, sterile α domain; SILAC, stable isotope labeling with amino acids in cell culture; siRNA, small interfering RNA; UBA domain, ubiquitin-associated domain; WT, wild type.

blocked at the stage of deeply invaginated clathrin-coated pits, whereas fluid-phase endocytosis, and possibly other forms of endocytosis, are preserved (Ferguson *et al.*, 2009). These cells represent an optimal experimental model to assess the effect of blocking clathrin-dependent internalization with an accumulation of normal endocytic clathrin coat assembly on signaling pathways.

Using these cells, we investigated the impact of the lack of dynamin on tyrosine phosphorylation, a major output of growth factor receptor signaling. The major change observed in these cells was a strong increase in the phosphorylation state of a 145-kDa band that we have identified as activated Cdc42-associated kinase (Ack; Manser *et al.*, 1993; Galisteo *et al.*, 2006). Interestingly, this robust increase is independent of growth factor receptor activation.

Ack (also called Ack1, Tnk2, or Pyk1) is a nonreceptor tyrosine kinase, which was reported to be activated by growth factors and a multiplicity of other extracellular stimuli. Ack was first identified as a Cdc42 effector (Manser *et al.*, 1993), forms a complex with Grb2 (Lev *et al.*, 1995), and is a negative regulator of epidermal growth factor receptor (EGFR) signaling (Hopper *et al.*, 2000; Yoo *et al.*, 2004; Galisteo *et al.*, 2006). The tyrosine kinase domain is flanked by domains responsible for protein–protein interactions: a sterile α domain (SAM domain) at the N-terminal side and several domains at the C-terminal side, including a Cdc42/Rac interacting-binding (CRIB) domain, a Ralt homology region, a proline-rich region, and a ubiquitin-associated domain (UBA domain). Ack2, originally reported to be a homologue of Ack1 (Yang and Cerione, 1997), was subsequently shown to be encoded by the same gene (Galisteo *et al.*, 2006). Relevant to its increased phosphorylation state in cells that lack dynamin (i.e., cells that accumulate clathrin-coated pits), Ack was reported to be localized at clathrin-coated pits and to directly bind clathrin heavy chain (CHC; Teo *et al.*, 2001; Yang *et al.*, 2001). This link to clathrin prompted us to examine the mechanisms leading to the increased phosphorylation state of Ack in dynamin DKO cells. We provide new evidence connecting Ack to endocytic clathrin coats and we report that its increased phosphorylation is dependent on its localization at clathrin-coated pits. Thus Ack represents a point of convergence between clathrin-mediated endocytosis and signal transduction.

RESULTS

Enhanced tyrosine phosphorylation of Ack in dynamin DKO cells

To determine the overall impact of blocking the fission reaction of clathrin-mediated endocytosis on tyrosine phosphorylation, we used anti-phosphotyrosine antibodies in immunofluorescence and Western blot experiments on wild-type (WT) cells (dnm1$^{flox/flox}$; dnm2 $^{flox/flox}$; Cre-Esr1$^{+/0}$ fibroblasts without 4-hydroxytamoxifen treatment) and dynamin DKO cells (the same cells with 4-hydroxytamoxifen addition). By immunofluorescence, prominent antiphosphotyrosine immunoreactivity was observed at the cell periphery, at sites of focal adhesions, in both cell lines. In DKO cells, however, a robust increase of punctate fluorescence signals throughout the cell surface was additionally observed relative to WT cells. Such fluorescence colocalized to a large extent with markers of the arrested, tubulated clathrin-coated pits previously described in these cells (Ferguson *et al.*, 2009) (Figure 1A). By Western blotting, the most consistent and clear difference observed in DKO cells was an increase in the phosphorylation states of a major band at 145 kDa (arrow in Figure 1B) and a minor band at 72 kDa (asterisk in Figure 1B).

To characterize the phosphoprotein at 145 kDa, we considered several potential candidate phosphoproteins with molecular weight in the range of 145 kDa. From these candidates, Western blotting of antiphosphotyrosine immunoprecipitates tentatively identified the band as Ack (Supplemental Figure S1). Ack is a nonreceptor tyrosine kinase (also known as Ack1, Tnk2, or Pyk1), which can undergo autophosphorylation upon activation. Interestingly, Ack is a clathrin-coated pit–associated protein (Teo *et al.*, 2001; Yang *et al.*, 2001) (see also Figure 4 later in the paper). As shown in Figure 1C, antiphosphotyrosine Western blot of anti-Ack immunoprecipitates generated from DKO cells revealed a strong increase in the signal of the Ack band in DKO cells despite a decrease in the total level of Ack, as shown by anti-Ack Western blotting (Figure 1C). Enhanced degradation of Ack

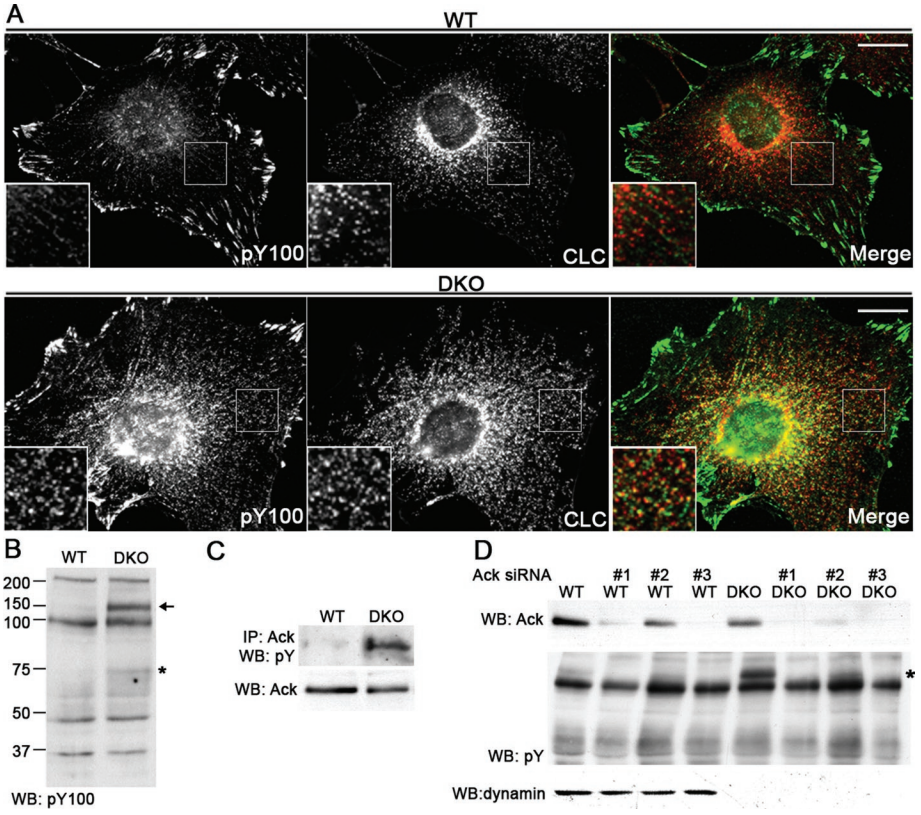

FIGURE 1: Increased phosphotyrosine immunoreactivity at clathrin-coated pits and enhanced tyrosine phosphorylation of Ack in dynamin DKO fibroblasts. (A) Two-color immunofluorescence staining with anti-phosphotyrosine (pY100) and anti-CLC antibodies revealed a robust increase of punctate phosphotyrosine signal at arrested clathrin-coated pits in DKO cells compared with WT cells. (B) Anti-phosphotyrosine (pY100) Western blotting (WB) of cell lysates revealed an increase in the phosphorylation state of a major band at 145 kDa (arrow), and a minor band at 72 kDa (asterisk) in DKO cells. (C) Anti-phosphotyrosine (pY100) WB of anti-Ack (Ab 880) immunoprecipitates (top) and total cell homogenates (bottom). (D) RNAi-induced knockdown of Ack (top, #1–#3 indicate three different siRNAs) in DKO cells resulted in almost complete disappearance of the phosphotyrosine immunoreactive band at 145 kDa (asterisk).

upon phosphorylation (activation) has been previously reported (Chan *et al.*, 2009; Lin *et al.*, 2010). The identification of the 145-kDa band as Ack was further confirmed by the near disappearance of the phosphotyrosine immunoreactive band at 145 kDa in DKO cell extracts depleted of Ack by prior immunodepletion using anti-Ack antibody (Figure S2) or in extracts obtained from cells in which Ack levels had been knocked down by small interfering siRNA (siRNA; Figure 1D). The siRNA experiment also resulted in the depletion of the 72-kDa band, raising the possibility that this band may represent an Ack fragment (degradation product) or a variant not recognized by our anti-Ack antibodies. The identity of this band was not investigated further in this study.

The enhanced phosphorylation state of Ack is growth factor independent

Ack was previously shown to be activated and autophosphorylated in response to a variety of signals, including growth factors (Galisteo *et al.*, 2006). Hence we next investigated whether the increased phosphorylation state of Ack was dependent on enhanced growth factor receptor signaling resulting from a block in the endocytosis of the signaling receptors, for instance EGFR. Both total levels of EGFR and levels of cell surface exposed EGFR, as reported by surface biotinylation experiments, were similar in WT and DKO cells (Figure S3), thus speaking against a role of impaired EGFR internalization in the increased phosphorylation of Ack. Note that, in contrast, cell surface levels of transferrin receptor, a protein the internalization of which is critically dependent on clathrin-mediated endocytosis (Dautry-Varsat, 1986; Nesterov *et al.*, 1999), were elevated in DKO cells (Figure S3), indicating that dynamin differentially affects the internalization of different receptors.

Stimulation of serum-starved WT and DKO cells with EGF (10 ng/ml) induced a strong and transient increase in the tyrosine-phosphorylation state of a 190-kDa band (arrows in Figure 2A), indicating EGFR responsiveness in these cells. In contrast, the tyrosine-phosphorylation state in DKO cells of the 145-kDa band (arrowhead in Figure 2A) and of the 72-kDa band (asterisk in Figure 2A) did not increase further above the increase already observed under serum starvation conditions (0-min condition in Figure 2A). The identity of the 145-kDa phosphorylated band as Ack was confirmed by anti-Ack Western blotting of antiphosphotyrosine immunoprecipitates (to reveal phospho-Ack) and total homogenates (to reveal total Ack) (Figure 2A). Similar results were obtained following EGF treatment at high doses (Figures 2B and S4). Because the rate of EGFR degradation was only partially affected by the lack of dynamin (Figure 2A, top blot), these experiments also indicate that dynamin-dependent endocytosis is not the sole route for receptor internalization toward degradation under our experimental conditions.

The enhanced phosphorylation state of Ack reflects an activated state

Upon activation, Ack *trans*-autophosphorylates itself at tyrosine residue 284 in the activation loop of the kinase domain, further increasing its kinase activity (Yokoyama and Miller, 2003; Lougheed *et al.*, 2004; Galisteo *et al.*, 2006). Besides the phospho site at Y284, phosphorylation of tyrosine at positions 533 and 874 have been identified in Ack from murine brain by phosphoproteomics (Ballif *et al.*, 2008). Two independent methods indicate that phosphorylation of Tyr284 of Ack contributes to the increase in total tyrosine phosphorylation of Ack observed in DKO cells. First, a phosphospecific antibody directed against this site (anti-pY284-Ack) produced an increased signal for the Ack band in anti-Ack immunoprecipitates from DKO cells, despite the lower overall amount of Ack in such immunoprecipitates (Figure 3A). Second, total tyrosine phosphorylation of exogenous Ack-GFP harboring a Y-to-A mutation at position 284 was decreased in dynamin knockout cells (Figure 3B). These findings suggest that Ack is activated in dynamin DKO cells.

The enhanced phosphorylation state of Ack is detected by a SILAC-based quantitative mass spectrometry analysis

As an independent approach to examine tyrosine phosphorylation in cells lacking dynamin, we used stable isotope labeling with amino acids in cell culture (SILAC)-based quantitative mass spectrometry. Extracts of cells grown in "light" and "heavy" SILAC medium (Ong *et al.*, 2003), respectively, were combined and digested with Lys-C protease. Phosphotyrosine peptides were enriched by affinity purification and analyzed on a LTQ-Orbitrap Discovery hybrid linear ion trap, searched against all mouse protein sequences, and filtered to a false discovery rate of 1% (Guo *et al.*, 2008).

We identified several phosphopeptides the levels of which were increased in DKO cells relative to WT (Table 1). In agreement with the Western blot results, one of the peptides the phosphorylation state of which was increased in dynamin DKO cells belongs to Ack. The lack of visualization of the other proteins detected by this method may be explained by their lower abundance. Interestingly, one protein in Table 1, Nck1, was reported to be an Ack binding protein (Galisteo *et al.*, 2006).

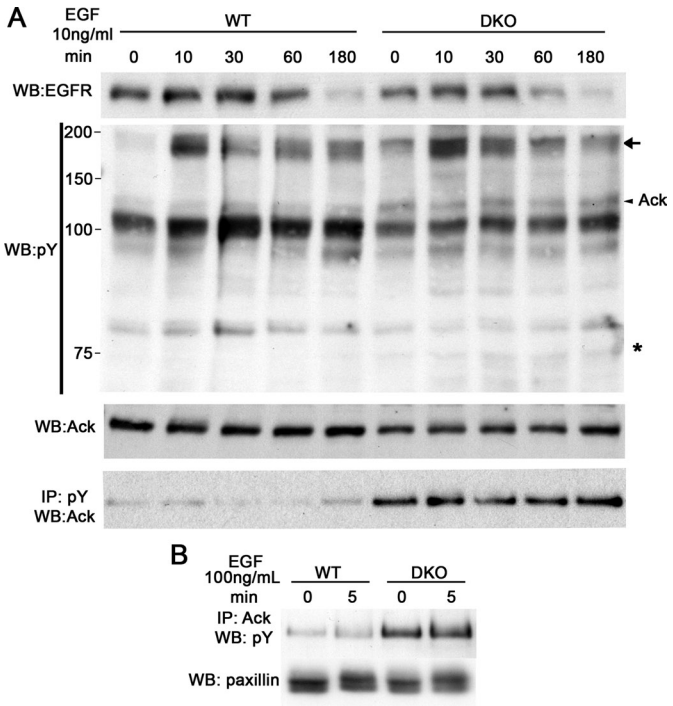

FIGURE 2: The increased phosphorylation of Ack is independent of growth factor stimulation. (A) Serum starved WT and DKO cells were stimulated with EGF at 10 ng/ml for the indicated time prior to lysis. Total cell homogenates were subjected to Western blotting using anti-EGFR, anti-phosphotyrosine, and anti-Ack antibodies. Anti-phosphotyrosine immunoprecipitates were generated and further analyzed by anti-Ack Western blotting. Note the enhanced phosphorylation of bands at 190 kDa (arrow) and 72 kDa (asterisk), and of Ack (arrowhead). (B) Serum-starved WT and DKO cells were lysed (0 min) or stimulated with EGF at high doses (100 ng/ml) for 5 min before lysis. Ack phosphorylation was examined by anti-phosphotyrosine (pY100) Western blotting of anti-Ack (Ab 880) immunoprecipitates. Anti-paxillin Western blots from total cell homogenates were used as loading controls.

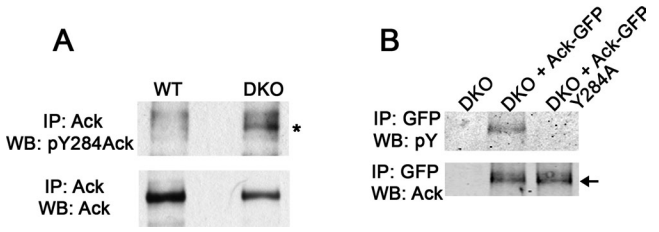

FIGURE 3: Increased phosphorylation of Ack at Tyr284 in DKO cells suggests an increased activation of the protein. (A) Western blotting of anti-Ack immunoprecipitates from DKO and WT cells using a phosphospecific antibody directed against pY284 of Ack (Ab 688, top) and anti-Ack (Ab 880, bottom) antibodies. Note that the global level of Ack in DKO cells is decreased. An asterisk marks pY284-Ack. (B) Anti-phosphotyrosine (Ab pY100, top) and anti-Ack Western blotting of anti-GFP immunoprecipitates from DKO cells expressing GFP fusions of WT Ack or of Ack harboring a Y-to-A mutation at position 284. An arrow indicates the Ack-GFP band.

Surprisingly, the upregulated Ack phosphopeptide we identified by SILAC contains tyrosine 533 and not the activation loop site tyrosine 284 (Figure 3). Although we did identify a phosphopeptide containing tyrosine 284, this phosphopeptide could not be quantified due to a low signal-to-noise ratio. Because overexpressed Ack in HEK293 cells is subject to autophosphorylation, we used these cells to identify all potential phosphorylated tyrosine residues in Ack. Immunopurified recombinant Ack-GFP from HEK293 cells was resolved by SDS–PAGE and the corresponding Ack-GFP band was cut out and analyzed by mass spectrometry. The identified phosphotyrosine residues are shown in Table 2. Both tyrosine 284 and tyrosine 533 were detected under these conditions, suggesting that both tyrosine residues are potential autophosphorylation sites. The most straightforward interpretation of our results is that, in DKO cells, Ack undergoes an increase in phosphorylation on at least these two sites.

Molecular interactions of Ack at endocytic clathrin-coated pits

The increase in the phosphorylation state of Ack in dynamin DKO cells (i.e., in cells with arrested and accumulated clathrin-coated pits) was of special interest. Ack was shown to be present at a subset of endocytic clathrin-coated pits (Teo *et al.*, 2001; Yang *et al.*, 2001), and to contain a (nonconventional) clathrin binding motif (clathrin box [Dell'Angelica, 2001]) (LIDFG, amino acids 584–588) that binds to the N-terminal β-propeller domain of clathrin heavy chain (CHC) (Figure 4B). Inspection of the Ack sequence revealed another potential clathrin box, LLSVE (amino acids 496–500), at the C-terminal side of the CRIB domain (Figure 4B). In fact, this motif has a negatively charged amino acid (glutamic acid) at position 5 and thus fits the classical clathrin box consensus (Dell'Angelica, 2001). The clathrin binding properties of these two motifs were confirmed by GST pulldown from rat brain homogenates using glutathione *S*-transferase (GST) fusions of Ack fragments (485–604) containing both motifs (Figure 4, B and C).

Mutations of either one of the two clathrin boxes (mutation of the bulky hydrophobic amino acids at positions 1 and 2 of the consensus into alanine) reduced but did not eliminate CHC binding in the GST pulldowns. In contrast, mutation of both clathrin boxes completely abolished CHC interactions (Figure 4C). The presence of two clathrin binding motifs has been found in other endocytic proteins, for instance, amphiphysin, the long isoform of arrestin 2, and OCRL (OculoCerebroRenal syndrome of Lowe) (Dell'Angelica, 2001; Miele *et al.*, 2004; Kang *et al.*, 2009; Mao *et al.*, 2009).

Mutation of both clathrin boxes partially impaired but did not completely block targeting of Ack-GFP to clathrin-coated pits in living cells (Figure S5), indicating the importance of other interactions for this localization. Indeed, besides binding directly to clathrin, Ack also binds other clathrin coat associated proteins, for example, amphiphysin (Chan *et al.*, 2009) and SNX9 (Lin *et al.*, 2002). Most likely, the formation and dissociation of these interactions in living cells is tightly orchestrated in space and time during the endocytic reaction. This multitude of interactions may explain our observation that high levels of Ack overexpression result in the formation of aggregates that include, besides Ack, clathrin (Figure 4D) and a variety of endocytic factors that function together with clathrin, including SNX9, dynamin, and epsin (Figure S6). Formation of these aggregates coincides with the arrest of clathrin-mediated endocytosis, as assessed by the uptake of transferrin (Figure S7), a protein cargo typically internalized by this pathway.

Phosphorylation of Ack is dependent on its localization at clathrin-coated pits

In agreement with the localization of Ack at clathrin-coated pits in WT cells, striking clathrin-coated pit localization was also observed

Protein	Description	Peptide sequence	Site	Fold change	n	$\log_2$ (H:L)
Tnk2/Ack	Activated CDC42 kinase 1	KPTY*DPVSEDPDPLSSDFK	Y533	2.06	2	1.04 ± 0.07
Rexo2	Oligoribonuclease, mitochondrial	HLHY*RIIDVSTVK	Y164	1.95	3	0.96 ± 0.25
Ptpn11	Tyrosine-protein phosphatase nonreceptor type 11	IQNTGDY*YDLYGGEK	Y62	1.59	3	0.67 ± 0.31
Ptpn11	Tyrosine-protein phosphatase nonreceptor type 11	GHEY*TNIK	Y547	1.75	3	0.81 ± 0.25
Nck1	noncatalytic region of tyrosine kinase adaptor protein 1	RKPSVPDTASPADDSFVDPGE-RLY*DLNMPAFVK	Y105	1.76	1	0.82
C230081A13Rik	Tyrosine-protein kinase–protein kinase SgK269	SSAIRY*QEVWTSSTSPRQK	Y528	1.64	3	0.71 ± 0.11

TABLE 1: Enhanced phosphotyrosine containing peptides in DKO cells identified by quantitative mass spectrometry. Phosphorylated tyrosine residues are indicated as Y*. Fold change is the average abundance ratio between the peptide in heavy medium (DKO) and light medium (WT); n = number of independent measurements. Log2 ratios of the fold change are included along with standard deviation measurements where available.

Ack peptide	Phosphotyrosine residue(s)
PTY*DPVSEDPDPLSSDFK	Y533
IGDFGLMRALPQNDDHY*VMQEHRK	Y284
Y*ATPQVIQAPGPR	Y842
VSSTHY*YLLPERPPYLER	Y874
VSSTHY*YLLPERPPYLERY*QR	Y874, Y887

TABLE 2: Phosphorylated tyrosine residues detected in Ack. Ack-GFP expressed in HEK293 was immunoprecipitated with Chromotek GFP-Trap beads and separated on SDS–PAGE gels. Gels were cut and subjected to mass spectrometry analysis. Detected tyrosine-phosphorylated peptides and the corresponding residue number of the phosphotyrosine are shown.

in DKO cells (Figure 5A, and Supplemental Movie S1), indicating that the enhanced state of phosphorylation of Ack did not compromise this localization. In fact, coimmunoprecipitation experiments from WT and DKO cells demonstrated an enrichment of clathrin and SNX9 in anti-Ack coimmunoprecipitates obtained from DKO cells (Figure S8). Such immunoprecipitates were also enriched in ubiquitinated proteins (Figure S8), which Ack may bind via its C-terminal UBA domain.

To determine whether the increased state of phosphorylation of Ack in dynamin DKO cells was dependent on the clathrin-coated pit localization of Ack, CHC expression was suppressed in DKO cells with two independent siRNA duplexes. CHC knockdown reversed the increase in the tyrosine phosphorylation state of Ack in DKO cells relative to WT cells, as demonstrated by anti-Ack Western blotting of antiphosphotyrosine immunoprecipitates, whereas the tyrosine phosphorylation state of c-Src was not affected (Figure 5B). These results strongly suggest that the increase in Ack phosphorylation observed in DKO cells is not simply the result of the endocytic defect due to the lack of dynamin—this block is expected to be enhanced by the additional absence of clathrin—but by the presence of Ack in assembled and arrested clathrin coats.

Because RNA interference (RNAi)-mediated knockdown of clathrin requires a chronic (multiple day) treatment, we complemented these studies with a pharmacological approach that results in the acute elimination of endocytic clathrin-coated pits: treatment with 2% 1-butanol (Boucrot *et al.*, 2006). In the presence of primary alcohols, phospholipase D generates phosphatidyl alcohols instead of phosphatidic acid, thus resulting in greatly reduced PI(4)P 5-kinase activity and, within minutes, in the depletion of $PI(4,5)P_2$. Because $PI(4,5)P_2$ is a critical cofactor in the assembly of clathrin-coated pits at the plasma membrane (Zoncu *et al.*, 2007), endocytic clathrin-coated pits of control cells disappear within a similar time frame.

When 2% 1-butanol was added to DKO cells expressing green fluorescent protein-clathrin light chain (GFP-CLC), a major decrease in the number of clathrin-coated pits was observed at 2 min (Figure 5D and Supplemental Movie S2) (pits did not completely disappear probably as a result of the increased stability of clathrin-coated pits in these cells). This effect was reversible as shown by observation of the cells following a 5 min washout after the original 2 min incubation with 1-butanol. Anti-Ack Western blot of antiphosphotyrosine immunoprecipitates from DKO cell homogenates revealed that 1-butanol treatment also produced a major decrease in the phosphorylation levels of the Ack band (to levels lower than in WT cells) and that this change was reversed by 1-butanol washout (Figure 5C). This result, which involves acute, rather than chronic, disruption of clathrin coats as in the case of clathrin knockdown, further supports the hypothesis that clathrin coat assembly is needed for the increased Ack phosphorylation in DKO cells.

Binding to an assembled clathrin lattice is not sufficient to enhance Ack phosphorylation

The data just shown do not discriminate between an effect due to assembled clathrin lattices versus an effect dependent on the formation of bona fide endocytic clathrin-coated pits. Thus we explored the effect on Ack phosphorylation in WT cells of an experimental protocol that induces membrane-independent clathrin assembly in the cortical region.

It was shown that exposure of cells to hypertonic sucrose (0.45 M) induces the rapid formation of small clathrin microcages in close proximity to the plasma membrane. These cages do not contain any membrane (Heuser and Anderson, 1989). In agreement with these previous observations, 30 min after addition of 0.45 M sucrose to WT mouse fibroblasts expressing red fluorescent protein (RFP)-CLC, a massive formation of new small clathrin spots, reflecting microcage formation, was observed (Figure 5E and Supplemental Movie S3). Ack-GFP is colocalized with these structures. Under this condition, however, the tyrosine phosphorylation state of Ack was not affected (Figure 5F), indicating that clathrin assembly and recruitment of Ack into these structures is not sufficient to activate Ack. Thus activation and tyrosine phosphorylation of Ack require its incorporation into a bona fide endocytic clathrin coat.

Activated Cdc42 is implicated in the increased phosphorylation of Ack

Ack contains a CRIB domain, and was identified as a specific effector of Cdc42, a small GTPase, which also functions as an activator of N-WASP-Arp2/3–dependent actin nucleation (Manser *et al.*, 1993; Yang and Cerione, 1997; Mott *et al.*, 1999). Furthermore, Ack was shown to be associated with, and activated by, active Cdc42 in living cells (Yang and Cerione, 1997), a finding that we have corroborated by detecting enhanced Ack phosphorylation in Cdc42-expressing cells (Figure 6A). Cdc42 has been implicated in clathrin-dependent endocytosis (Hussain *et al.*, 2001). Accordingly, we have previously demonstrated that downstream effectors of Cdc42, N-WASP, Arp2/3, and actin are enriched around the deeply invaginated and tubulated neck of arrested endocytic clathrin-coated pits in dynamin DKO cells (Ferguson *et al.*, 2009). We further show here that factors that act upstream of Cdc42, the Cdc42 guanine-nucleotide exchange factor (GEF) intersectin-L (Hussain *et al.*, 2001), and another Cdc42 GEF, the dynamin binding protein Tuba (Salazar *et al.*, 2003; Cestra *et al.*, 2005), are strongly localized at clathrin-coated pits in DKO cells (Figure S9, A and B).

To determine whether Cdc42 activity plays a role in the increased tyrosine phosphorylation of Ack in dynamin DKO cells, the effect of Cdc42 knockdown was tested. Two distinct siRNAs both independently achieved a major down-regulation of Cdc42 levels as determined by Western blotting (Figure 6B). Further confirming the loss of Cdc42 function in these cells, the accumulation of actin at the neck of arrested endocytic clathrin-coated pits was no longer observed, as shown by phalloidin staining for F-actin (Figure 6C). In cells transfected with either of the two Cdc42 siRNA oligos, the increase in tyrosine phosphorylation of Ack was attenuated relative to control siRNA-transfected cells (Figure 6B), indicating a role of Cdc42 on the phosphorylation of Ack at clathrin-coated pits.

Because Cdc42 stimulates actin nucleation, assembled actin could in principle synergize with the direct binding of Cdc42 to Ack in triggering Ack activation and phosphorylation. In dynamin DKO

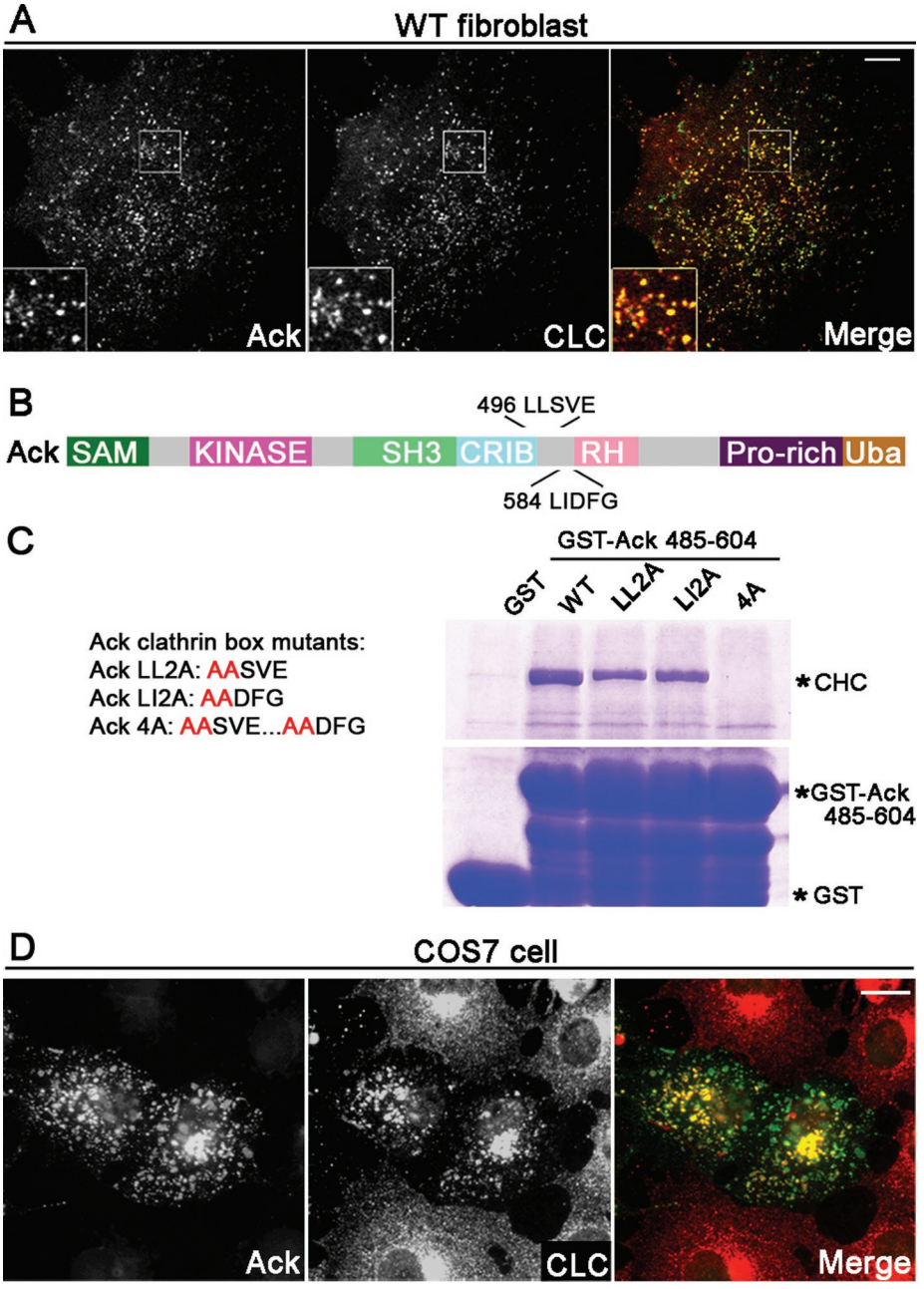

FIGURE 4: Ack is localized at clathrin-coated pits and contains two clathrin binding motifs. (A) Double immunofluorescence imaging shows that Ack-GFP colocalizes with RFP-CLC in WT mouse fibroblasts. Scale bar is 10 μm. (B) Domain structure of Ack. Ack contains two clathrin binding motifs, LLSVE and LIDFG. (C) GST pulldown from rat brain lysates using GST fusion of a WT Ack fragment comprising the two clathrin binding motifs (amino acids 485–604), or of the same fragment containing mutations in the two clathrin boxes, as indicated on the left. Coomassie blue–stained SDS–PAGE gels of the bound material are shown. Mutations at either single clathrin box reduced CHC binding, whereas mutation of both clathrin boxes abolished binding. (D) Strong overexpression of Ack-GFP in COS-7 cells generated aggregates that contain both Ack and endogenous clathrin as shown by immunofluorescence with anti-CLC antibody. Scale bar is 10 μm.

cells, inhibition of actin polymerization with latrunculin B results within 90 s in a reversible loss of actin at the tubular neck of clathrin-coated pits and in the collapse of the tubules, whereas clathrin coats are preserved (Ferguson *et al.*, 2009). Anti-Ack Western blotting of antiphosphotyrosine immunoprecipitates generated from DKO cells treated with latrunculin B revealed that this treatment did not affect the phosphorylation level of the Ack band (Figure 6D). Thus Ack phosphorylation is independent of actin nucleation.

DISCUSSION

We report here that a major effect of blocking clathrin-mediated endocytosis at the stage of deeply invaginated clathrin-coated pits is an increase of the tyrosine phosphorylation state of the nonreceptor tyrosine kinase Ack, a clathrin-coated pit associated protein. This increase is due at least in part to the phosphorylation of tyrosine at position 284, a covalent modification known to reflect activation of the kinase by autophosphorylation. We further show that this increase is critically dependent on the localization of Ack at clathrin-coated pits and on Cdc42 activation, consistent with the identification of Ack as a Cdc42 effector. Thus our study suggests that Ack represents an important point of convergence between the clathrin-dependent endocytic machinery and signal transduction. It further reveals a link between progression of clathrin-coated pits to clathrin-coated vesicles and an activation–deactivation cycle of Ack.

Ack was shown previously to be localized at clathrin-coated pits and to interact, directly or indirectly, with clathrin (via a clathrin box), as well as with several other endocytic proteins, including amphiphysin (Chan *et al.*, 2009), SNX9 (Lin *et al.*, 2002), and AP-2 (Chan *et al.*, 2009). We have confirmed this link to endocytic clathrin coats, identified a new clathrin box, and shown that both clathrin boxes contribute to clathrin binding. We have also shown that the increase in Ack phosphorylation observed in DKO cells requires the formation of endocytic clathrin-coated pits and the assembly of Ack into the pits.

The multiplicity of binding sites for endocytic and signaling proteins in Ack (a SAM domain, clathrin boxes, the CRIB domain, a Ralt homology region, Src homology 3 domain binding sites, and UBA (ubiquitin associated domain), suggests the existence of inter- and intramolecular regulatory mechanisms to control its actions. These mechanisms may include activation mechanisms, such as dimerization, and relief of autoinhibitory intramolecular constraints that are regulated by intermolecular interactions and by phosphorylation. For example, the newly identified second clathrin box of Ack (LLSVE) resides adjacent to the C-terminal side of the Cdc42 effector domain, the CRIB domain. Based on studies of other CRIB domain–containing proteins, the CRIB domain can also be engaged in intramolecular autoinhibitory interactions (Kim *et al.*, 2000; Lei *et al.*, 2000), suggesting that binding to clathrin may influence regulation of Ack's kinase activity. Additional intramolecular interactions may occur. For example, the autoinhibitory binding in the yeast

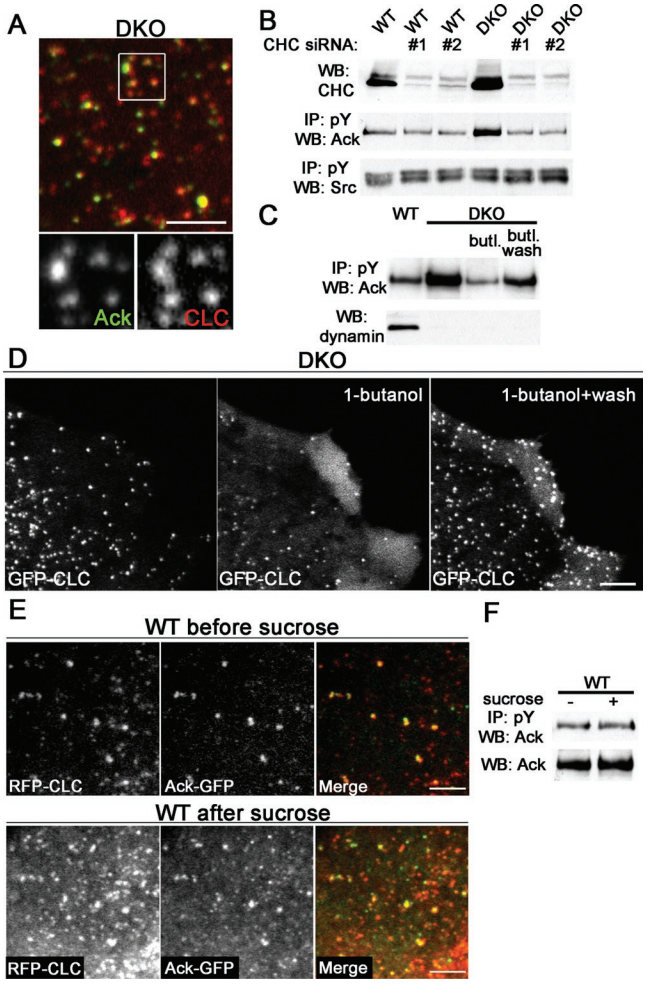

FIGURE 5: Enhanced phosphorylation of Ack in DKO cells is dependent on its localization at clathrin-coated pits. (A) A dual color image of DKO cells expressing Ack-GFP and RFP-CLC (top) reveals the presence of Ack-GFP at clathrin-coated pits. The separate GFP and RFP channels corresponding to the field indicated by a white square are shown at higher magnification (bottom). (B) CHC knockdown in DKO cells abolished the increase of Ack phosphorylation, as shown by anti-phosphotyrosine (pY100) Western blotting of anti-Ack immunoprecipitates. Anti-c-Src Western blot of anti-pY immunoprecipitates was used as a control. (C) Disruption of clathrin-coated pits in DKO cells by acute treatment with 2% 1-butanol for 2 min resulted in reduced Ack phosphorylation levels. The increased phosphorylation of Ack in DKO cells recovered within 5 min after washing away 1-butanol. (D) Visualization of the reversible disruption of clathrin-coated pits by 1-butanol in DKO cells. DKO cells were transiently transfected with GFP-CLC and imaged by spinning disc confocal microscopy. Images taken before treatment, 2 min after 2% 1-butanol treatment, and 5 min after washing away 1-butanol are shown. Scale bar is 5 μm. (E) WT fibroblasts transiently expressing Ack-GFP and RFP-CLC were treated with 0.45 M sucrose. Images taken before and after treatment are shown. Scale bar is 5 μm. (F) Hypertonic treatment with sucrose (+) on WT fibroblasts did not induce increased phosphorylation of Ack, as shown by anti-phosphotyrosine (pY100) Western blotting of anti-Ack immunoprecipitates.

protein Sla1 between its N-terminal SAM domain and a clathrin box (Di Pietro *et al.*, 2010) raises the possibility of a similar interaction between the SAM domain of Ack and one of its clathrin boxes. The property of highly overexpressed Ack to induce aggregates containing many of its interactors (and, as a consequence, to block clathrin-mediated endocytosis) most likely reflects a disruption of the physiological interplay of these regulatory mechanisms. It will be of interest to determine whether the increased phosphorylation state of Ack in dynamin DKO cells simply reflects enhanced activation due to accumulation of upstream factors, such as clathrin and active Cdc42, and/or a defect in the activity of phosphatases that are activated during the normal progression of clathrin-coated pits toward fission from the plasma membrane.

Several protein–protein interactions of Ack link it to growth factor receptor signaling. Ack directly binds to EGFR adaptors, such as Grb2 or Nck (Lev *et al.*, 1995; Galisteo *et al.*, 2006), and its C-terminal region contains a RALT domain. The RALT domain of MIG6, a protein that contributes to the endocytosis of EGFR by linking it to the clathrin adaptor AP-2 and to the endocytic factor intersectin (Frosi *et al.*, 2010), directly binds and inhibits the EGFR kinase domain (Hackel *et al.*, 2001; Anastasi *et al.*, 2005; Xu *et al.*, 2005; Zhang *et al.*, 2007). Furthermore, genetic evidence in *Caenorhabditis elegans* points to a role of Ack (ARK-1) as a negative regulator of early steps in the EGFR (let-23) signaling pathway in a Grb2 (sem-5)-dependent manner (Hopper *et al.*, 2000). Interestingly, other negative regulators of this pathway in *C. elegans* include components of the clathrin-dependent endocytic machinery, such as the μ2 subunit of the AP-2 complex (dpy-23) and SNX9 (lst-4) (Yoo *et al.*, 2004). Thus the direct and indirect interactions, both biochemical and genetic, of Ack with endocytic factors raise the possibility that the inhibitory effect of Ack on the action of EGFR signaling may be mediated by a more general action of Ack on the endocytic machinery. Such regulation may explain a lack of increase in global Ack phosphorylation in response to EGF stimulation, as well as results from studies in *Drosophila* and in mammalian cells indicating that Ack acts in other signaling pathways as well (Yang and Cerione, 1997; Worby *et al.*, 2002; Galisteo *et al.*, 2006).

A pool of endogenous Ack is constitutively phosphorylated, independent of growth factor stimulation (Galisteo *et al.*, 2006), also suggesting constitutive functions of Ack. The increase in the phosphorylation state of Ack in DKO cells may indeed represent an increase of this pool in DKO cells as a result of a disruption of the assembly–disassembly cycle of clathrin-coated pits. Such an increase, resulting from an impairment of clathrin-coated pit release, may unmask the occurrence of a phosphorylation reaction that is only transient in WT cells.

A precise elucidation of the role of Ack in signaling and endocytic clathrin coat dynamics, and the relative contributions to these actions of its tyrosine kinase activity and/or scaffolding properties, is an important priority for future studies. Because mutations in the coding sequence of Ack (Ruhe *et al.*, 2007) and abnormal expression of Ack (van der Horst *et al.*, 2005) have been reported in several types of cancer, these studies may have important implications for cancer research.

MATERIALS AND METHODS

Cell cultures

The generation of tamoxifen-inducible dynamin conditional knockout mouse fibroblasts (dnm1$^{flox/flox}$; dnm2 $^{flox/flox}$; Cre-Esr1$^{+/0}$) was previously described (Ferguson *et al.*, 2009). Dynamin deletion was acutely achieved in these cells by two sequential 24-h incubations with 3 μM 4-hydroxytamoxifen (Sigma, St. Louis, MO). Cells were generally used for experiments between 6 and 9 d after initiating tamoxifen treatment. For growth factor stimulation, fibroblasts were serum starved for 16–24 h prior to addition of human EGF (Millipore/Upstate, Billerica, MA) at indicated concentrations and for indicated times prior to lysis.

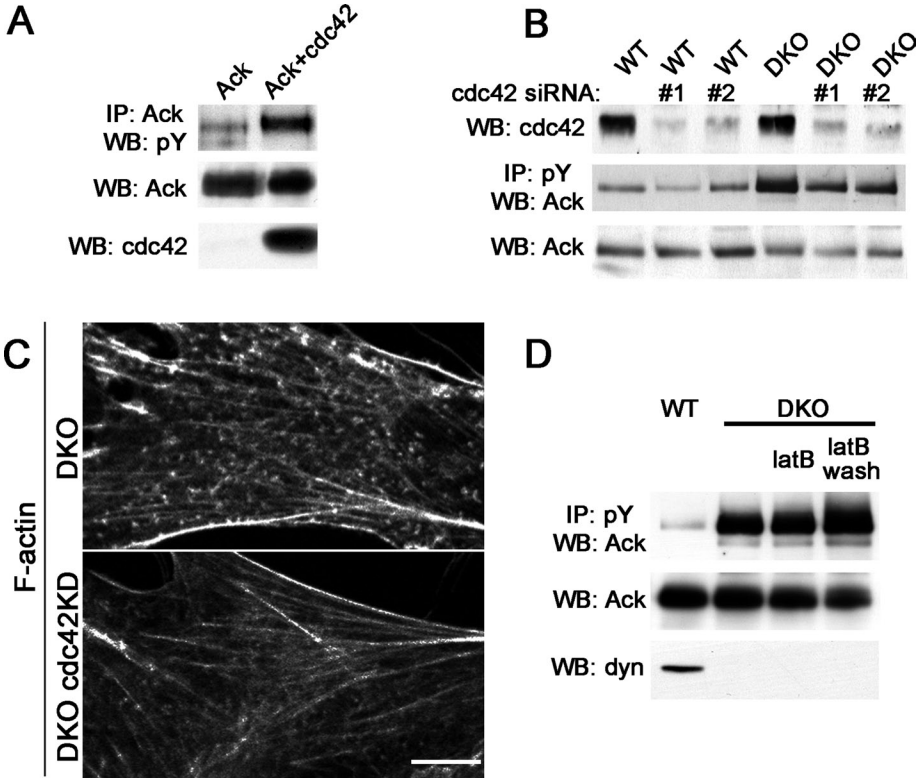

FIGURE 6: Activated Cdc42 is implicated in the increased phosphorylation of Ack in DKO cells. (A) COS-7 cells were transfected with Ack alone or with both Ack and Cdc42. Overexpression of Cdc42 led to enhanced Ack phosphorylation, as revealed by anti-phosphotyrosine Western blotting (pY100) of anti-Ack immunoprecipitates. (B and C) RNAi-induced depletion of Cdc42 in DKO cells reduced the accumulation of actin (phalloidin staining) at the arrested endocytic pits that were present in these cells (C), and attenuated the increased tyrosine phosphorylation of Ack (B). Scale bar in C is 10 μm. (D) Acute inhibition of actin polymerization in DKO cells with latrunculin B did not affect the phosphorylation levels of Ack, as shown by anti-Ack Western blotting of anti-phosphotyrosine (4G10) immunoprecipitates. Dyn = dynamin.

HEK293T cells and COS cells were purchased from American Type Culture Collection (ATCC; Manassas, VA). Cells were grown in DMEM + 10% fetal bovine serum + 1% penicillin/streptomycin. Cell culture reagents were purchased from Invitrogen (Carlsbad, CA).

Plasmids, antibodies, and chemical reagents

Cloning of Ack cDNA and preparation of Ack-GFP and Ack Y284A-GFP plasmids were previously described (Galisteo *et al.*, 2006). Ack-GFP mutants bearing mutations in either of the two clathrin boxes (LI2A and LL2A), or in both clathrin boxes (4A), were generated subsequently using the Quikchange site-directed mutagenesis method (Stratagene, La Jolla, CA). The region (amino acids 485–604) of Ack containing clathrin interaction sites (clathrin boxes) was fused to GST by insertion into pGEX-6P-1 plasmid (GE/Amersham, Pittsburgh, PA). GST-Ack (amino acids 485–604) constructs bearing the mutation in either of the two clathrin boxes, or both, were generated subsequently using the Quikchange site-directed mutagenesis strategy (Stratagene, La Jolla, CA). GFP-CLC was a gift from James Keen (Thomas Jefferson University, Philadelphia, PA), and mRFP-CLC was generated in the laboratory of Pietro De Camilli.

Antibodies for Western blotting, immunoprecipitation, and immunofluorescence were obtained from the following sources: phosphotyrosine pY100 (Cell Signaling, Beverly, MA), phosphotyrosine 4G10 (Millipore, Billerica, MA), paxillin (clone 349; BD Biosciences, San Jose, CA), EGFR (Rockland, Gilbertsville, PA), GFP (ab290; Abcam, Cambridge, MA), CHC (clone TD1; ATCC), Cdc42 (Cell Signaling, Beverly, MA), pan-dynamin (clone 41; BD Biosciences, San Jose, CA), transferrin receptor (Invitrogen/Zymed, Carlsbad, CA), ubiquitin (FK2; Enzo/BIOMOL, Farmingdale, NY), dynamin 2 (Santa Cruz Biotechnology, Santa Cruz, CA), epsin 1 (R-20; Santa Cruz Biotechnology) and CLC (MIllipore, Billerica, MA). Ack (ab880) and phospho-specific pY284 (ab 688) Ack antibodies were generated in the laboratory of Joseph Schlessinger (Yale University). SNX9 antibody was generated in the laboratory of Pietro De Camilli. Chromotek GFP-Trap (Allele Biotech, San Diego, CA) was used for anti-GFP immunoprecipitation experiments. Alexa Fluor 488 phalloidin (Invitrogen, Carlsbad, CA) was used for staining F-actin in cells.

The following chemicals were used for pharmacological treatments: 1-butanol (J.T. Baker, Phillipsburg, NJ), sucrose (Sigma, St. Louis, MO), and latrunculin B (Calbiochem, San Diego, CA).

Immunoprecipitation and Western blotting

Western blotting was performed by standard methods. Total cell lysates were prepared in a lysis buffer containing 25 mM Tris, pH 7.5, 150 mM NaCl, 1% SDS, 1 mM EDTA, Complete Protease Inhibitor Cocktail (Roche Diagnostics, Indianapolis, IN), and PhosSTOP phosphatase inhibitor cocktail (Roche Diagnostics, Indianapolis, IN). The lysis buffer for immunoprecipitation experiments contained 1% Triton X-100 with or without 0.1% SDS.

Immunofluorescence

Cells were grown on glass coverslips, fixed with 4% paraformaldehyde in 0.1 M sodium phosphate, pH 7.2, washed with 50 mM NH_4Cl, pH 7.2, and blocked and permeabilized with PBS + 3% bovine serum albumin + 0.1% Triton X100. Subsequent primary and secondary antibody incubations were also performed in this buffer. Coverslips were finally mounted in Prolong Gold mounting medium (Invitrogen, Carlsbad, CA). Samples were imaged with a Zeiss Axioplan 2 microscope using a Plan-Apochromatic 40× objective and a Hamamatsu (Bridgewater, NJ) ORCA II digital camera under the control of MetaMorph software (Molecular Devices, Sunnyvale, CA) (for images in Figures 5E and S6) or by spinning disk confocal microscopy using the method described below (for images in Figures 1; 4A; 5, A and D; 6; S5; S7; and S9).

Transfection methods

Fibroblasts were electroporated with the Amaxa Nucleofection method (kit R, program T-20) and grown for 24 h before assays. HEK293 and COS-7 cells were transfected with either lipofectamine 2000 (Invitrogen) or Fugene 6 (Roche).

Spinning disk confocal microscopy and total internal reflection fluorescence microscopy

Spinning disk confocal microscopy was performed as previously described (Ferguson *et al.*, 2009). Total internal fluorescence microscopy was performed using a Nikon Ti-E Eclipse inverted

microscope fitted with Apo TIRF 100× N.A. 1.49 oil objective, driven by Andor iQ software (Andor Technologies, Belfast, Ireland). Images were acquired with a back-illuminated Andor iXon 897 EMCCD camera (512 × 512, 14 bit; Andor Technologies). Cells were imaged in two channels by sequential excitation at 0.25 Hz. Postacquisition image analysis was performed using ImageJ software (1.43u; National Institutes of Health, Bethesda, MD).

siRNA transfection and knockdown

RNAi-based knockdown of CHC, Cdc42, and Ack in mouse fibroblasts was modified from methods described previously (Ferguson *et al.*, 2009). Specifically, cells were transfected twice with siRNA oligos (IDT, Coralville, IA) using RNAiMAX (Invitrogen) at 1 and 4 d after initiating 4-hydroxytamoxifen or vehicle treatment, and were used for experiments 2 d after the second transfection.

siRNA sequences were as follows:

Control, 5′-CUUCCUCUCUUUCUCUCCCUUGGA-3′ annealed to 5′-UCACAAGGGAGAGAAAGAGAGGAAGGA-3′,
CHC #1, 5′-CCAAUGUACCUAAUAAAGUCAUCCA-3′ annealed to 5′-UGGAUGACUUUAUUAGGUACAUUGGCC-3′,
CHC #2, 5′-GGAAAGUUACAUAUCAUUGAAGUTG-3′ annealed to 5′-CAACUUCAAUGAUAUGUAACUUUCCUC-3′,
Cdc42 #1, 5′-GCUGAGGACAAGAUCUAAUUUGAAA-3′ annealed to 5′-UUUCAAAUUAGAUCUUGUCCUCAGCUU-3′, and
Cdc42 #2, 5′-GACUAAUUCAGAUUGUCAAAGCUGC-3′ annealed to 5′-GCAGCUUUGACAAUCUGAAUUAGUCUG-3′,
Ack #1, 5′-CCACUAUGUCAUGCAAGAACACCGC-3′ annealed to 5′-GCGGUGUUCUUGCAUGACAUAGUGGUC-3′,
Ack #2, 5′-CUCAGGAAAUACUGUUGUAGCUGCACC-3′ annealed to 5′-UGCAGCUACAACAGUAUUUCCUGAG-3′,
Ack #3, 5′-GCCUGAAGACACGGACUUUCUCCCA-3′ annealed to 5′-UGGGAGAAAGUCCGUGUCUUCAGGCUC-3′.

PhosphoScan-SILAC analysis of tyrosine phosphorylation in DKO cells

Equal numbers of DKO fibroblasts and WT controls were grown in heavy (supplemented with L-lysine [$^{13}C_6$]) and light (supplemented with regular L-lysine) SILAC DMEM medium (Thermo Fisher Pierce, Rockford, IL). The cells were grown for at least five cell divisions in heavy medium to ensure sufficient incorporation before adding 4-hydroxytamoxifen to generate DKO cells. Cell lysis and phosphopeptide enrichment were performed according to the PhosphoScan kit protocol (Cell Signaling, Beverly, MA), except that the lysates were subjected to digestion using Lys-C protease (lysyl endopeptidase; Wako, Richmond, VA). Phosphopeptides were analyzed by liquid chromatography tandem mass spectrometry (LC-MS/MS) on an LTQ-Orbitrap Discovery hybrid linear ion trap (Thermo Fisher Pierce, Rockford, IL) using a top-10 method. For each scan cycle, one high-resolution full MS scan was acquired in the Orbitrap mass analyzer, and up to 10 parent ions were chosen based on intensity for MS/MS analysis in the linear ion trap.

MS/MS spectra were searched using the SEQUEST (Eng *et al.*, 1994) algorithm (v.27, rev.13) against a composite mouse database (IPI v3.60) and its reversed complement. Search parameters specified lys-C digestion, a mass tolerance of 25 ppm, a static modification of 57.02146 Da on cysteine, and dynamic modifications of 15.99491 Da on methionine, 6.02013 Da on lysine, and 79.96633 Da on serine, threonine, and tyrosine. Search results were filtered to a 1% peptide false discovery rate by restricting the mass tolerance window, and setting thresholds for Xcorr and dCn. For all resulting peptides, a heavy/light abundance ratio was calculated using Vista. The data were further filtered to require a signal-to-noise ratio ≥ 3 for both heavy and light versions of each peptide. The confidence of phosphorylation site assignment was measured by applying the Ascore algorithm (Beausoleil *et al.*, 2006).

Phosphorylation site determination on Ack-GFP

HEK293 cells were transfected with Ack-GFP and were lysed as described previously. Overexpressed Ack-GFP was immunopurified using Chromotek GFP-Trap agarose beads (Allele Biotech, San Diego, CA), separated by SDS–PAGE, and stained with Coomassie blue. The band corresponding to Ack-GFP was cut out, extracted, digested, and subjected to LC-MS/MS analysis as previously described. The spectra were searched with no enzyme specified against the Ack-GFP sequence only and filtered by requiring lys-C digestion and by restricting the mass tolerance window to ±3 ppm. All reported peptides were identified multiple times.

ACKNOWLEDGMENTS

We thank Frank Wilson, Lijuan Liu, and Louise Lucast for superb technical assistance and Min Wu and Michelle Pirruccello for discussions. This work was supported in part by the G. Harold and Leila Y. Mathers Charitable Foundation; the W.M. Keck Foundation; NIH grants R37NS036251, P30-DK45735, and P30-DA018343; a NARSAD Distinguished Investigator Award (to P.D.C.); as well as NIH grants R01-AR051448, R01-AR051886, and P50-AR054086 (to J.S).

REFERENCES

Anastasi S, Sala G, Huiping C, Caprini E, Russo G, Iacovelli S, Lucini F, Ingvarsson S, Segatto O (2005). Loss of RALT/MIG-6 expression in ERBB2-amplified breast carcinomas enhances ErbB-2 oncogenic potency and favors resistance to Herceptin. Oncogene 24, 4540–4548.

Ballif BA, Carey GR, Sunyaev SR, Gygi SP (2008). Large-scale identification and evolution indexing of tyrosine phosphorylation sites from murine brain. J Proteome Res 7, 311–318.

Beausoleil SA, Villen J, Gerber SA, Rush J, Gygi SP (2006). A probability-based approach for high-throughput protein phosphorylation analysis and site localization. Nat Biotechnol 24, 1285–1292.

Boucrot E, Saffarian S, Massol R, Kirchhausen T, Ehrlich M (2006). Role of lipids and actin in the formation of clathrin-coated pits. Exp Cell Res 312, 4036–4048.

Ceresa BP, Schmid SL (2000). Regulation of signal transduction by endocytosis. Curr Opin Cell Biol 12, 204–210.

Cestra G, Kwiatkowski A, Salazar M, Gertler F, De Camilli P (2005). Tuba, a GEF for CDC42, links dynamin to actin regulatory proteins. Methods Enzymol 404, 537–545.

Chan W, Tian R, Lee YF, Sit ST, Lim L, Manser E (2009). Down-regulation of active ACK1 is mediated by association with the E3 ubiquitin ligase Nedd4–2. J Biol Chem 284, 8185–8194.

Dautry-Varsat A (1986). Receptor-mediated endocytosis: the intracellular journey of transferrin and its receptor. Biochimie 68, 375–381.

Dell'Angelica EC (2001). Clathrin-binding proteins: got a motif? Join the network. Trends Cell Biol 11, 315–318.

Di Fiore PP, De Camilli P (2001). Endocytosis and signaling. An inseparable partnership. Cell 106, 1–4.

Di Pietro SM, Cascio D, Feliciano D, Bowie JU, Payne GS (2010). Regulation of clathrin adaptor function in endocytosis: novel role for the SAM domain. EMBO J 29, 1033–1044.

Eng JK, McCormack AL, Yates Iii JR (1994). An approach to correlate tandem mass spectral data of peptides with amino acid sequences in a protein database. J Am Soc Mass Spectrom 5, 976–989.

Ferguson SM *et al.* (2009). Coordinated actions of actin and BAR proteins upstream of dynamin at endocytic clathrin-coated pits. Dev Cell 17, 811–822.

Frosi Y, Anastasi S, Ballaro C, Varsano G, Castellani L, Maspero E, Polo S, Alema S, Segatto O (2010). A two-tiered mechanism of EGFR inhibition by RALT/MIG6 via kinase suppression and receptor degradation. J Cell Biol 189, 557–571.

Galisteo ML, Yang Y, Urena J, Schlessinger J (2006). Activation of the nonreceptor protein tyrosine kinase Ack by multiple extracellular stimuli. Proc Natl Acad Sci USA 103, 9796–9801.
Guo A *et al*. (2008). Signaling networks assembled by oncogenic EGFR and c-Met. Proc Natl Acad Sci USA 105, 692–697.
Hackel PO, Gishizky M, Ullrich A (2001). Mig-6 is a negative regulator of the epidermal growth factor receptor signal. Biol Chem 382, 1649–1662.
Heuser JE, Anderson RG (1989). Hypertonic media inhibit receptor-mediated endocytosis by blocking clathrin-coated pit formation. J Cell Biol 108, 389–400.
Hopper NA, Lee J, Sternberg PW (2000). ARK-1 inhibits EGFR signaling in C. elegans. Mol Cell 6, 65–75.
Hussain NK *et al*. (2001). Endocytic protein intersectin-l regulates actin assembly via Cdc42 and N-WASP. Nat Cell Biol 3, 927–932.
Kang DS, Kern RC, Puthenveedu MA, von Zastrow M, Williams JC, Benovic JL (2009). Structure of an arrestin2-clathrin complex reveals a novel clathrin binding domain that modulates receptor trafficking. J Biol Chem 284, 29860–29872.
Kim AS, Kakalis LT, Abdul-Manan N, Liu GA, Rosen MK (2000). Autoinhibition and activation mechanisms of the Wiskott-Aldrich syndrome protein. Nature 404, 151–158.
Lei M, Lu W, Meng W, Parrini MC, Eck MJ, Mayer BJ, Harrison SC (2000). Structure of PAK1 in an autoinhibited conformation reveals a multistage activation switch. Cell 102, 387–397.
Lemmon MA, Schlessinger J (2010). Cell signaling by receptor tyrosine kinases. Cell 141, 1117–1134.
Lev S, Moreno H, Martinez R, Canoll P, Peles E, Musacchio JM, Plowman GD, Rudy B, Schlessinger J (1995). Protein tyrosine kinase PYK2 involved in Ca(2+)-induced regulation of ion channel and MAP kinase functions. Nature 376, 737–745.
Lin Q, Lo CG, Cerione RA, Yang W (2002). The Cdc42 target ACK2 interacts with sorting nexin 9 (SH3PX1) to regulate epidermal growth factor receptor degradation. J Biol Chem 277, 10134–10138.
Lin Q, Wang J, Childress C, Sudol M, Carey DJ, Yang W (2010). HECT E3 ubiquitin ligase Nedd4–1 ubiquitinates ACK and regulates epidermal growth factor (EGF)-induced degradation of EGF receptor and ACK. Mol Cell Biol 30, 1541–1554.
Lougheed JC, Chen RH, Mak P, Stout TJ (2004). Crystal structures of the phosphorylated and unphosphorylated kinase domains of the Cdc42-associated tyrosine kinase ACK1. J Biol Chem 279, 44039–44045.
Manser E, Leung T, Salihuddin H, Tan L, Lim L (1993). A non-receptor tyrosine kinase that inhibits the GTPase activity of p21cdc42. Nature 363, 364–367.
Mao Y, Balkin DM, Zoncu R, Erdmann KS, Tomasini L, Hu F, Jin MM, Hodsdon ME, De Camilli P (2009). A PH domain within OCRL bridges clathrin-mediated membrane trafficking to phosphoinositide metabolism. EMBO J 28, 1831–1842.
Miaczynska M, Pelkmans L, Zerial M (2004). Not just a sink: endosomes in control of signal transduction. Curr Opin Cell Biol 16, 400–406.
Miele AE, Watson PJ, Evans PR, Traub LM, Owen DJ (2004). Two distinct interaction motifs in amphiphysin bind two independent sites on the clathrin terminal domain beta-propeller. Nat Struct Mol Biol 11, 242–248.
Mott HR, Owen D, Nietlispach D, Lowe PN, Manser E, Lim L, Laue ED (1999). Structure of the small G protein Cdc42 bound to the GTPase-binding domain of ACK. Nature 399, 384–388.
Nesterov A, Carter RE, Sorkina T, Gill GN, Sorkin A (1999). Inhibition of the receptor-binding function of clathrin adaptor protein AP-2 by dominant-negative mutant mu2 subunit and its effects on endocytosis. EMBO J 18, 2489–2499.
Ong SE, Foster LJ, Mann M (2003). Mass spectrometric-based approaches in quantitative proteomics. Methods 29, 124–130.
Ruhe JE *et al*. (2007). Genetic alterations in the tyrosine kinase transcriptome of human cancer cell lines. Cancer Res 67, 11368–11376.
Salazar MA, Kwiatkowski AV, Pellegrini L, Cestra G, Butler MH, Rossman KL, Serna DM, Sondek J, Gertler FB, De Camilli P (2003). Tuba, a novel protein containing bin/amphiphysin/Rvs and Dbl homology domains, links dynamin to regulation of the actin cytoskeleton. J Biol Chem 278, 49031–49043.
Sorkin A, von Zastrow M (2009). Endocytosis and signalling: intertwining molecular networks. Nat Rev Mol Cell Biol 10, 609–622.
Teo M, Tan L, Lim L, Manser E (2001). The tyrosine kinase ACK1 associates with clathrin-coated vesicles through a binding motif shared by arrestin and other adaptors. J Biol Chem 276, 18392–18398.
Van Der Horst EH *et al*. (2005). Metastatic properties and genomic amplification of the tyrosine kinase gene ACK1. Proc Natl Acad Sci USA 102, 15901–15906.
Worby CA, Simonson-Leff N, Clemens JC, Huddler D Jr, Muda M, Dixon JE (2002). Drosophila Ack targets its substrate, the sorting nexin DSH3PX1, to a protein complex involved in axonal guidance. J Biol Chem 277, 9422–9428.
Xu D, Makkinje A, Kyriakis JM (2005). Gene 33 is an endogenous inhibitor of epidermal growth factor (EGF) receptor signaling and mediates dexamethasone-induced suppression of EGF function. J Biol Chem 280, 2924–2933.
Yang W, Cerione RA (1997). Cloning and characterization of a novel Cdc42-associated tyrosine kinase, ACK-2, from bovine brain. J Biol Chem 272, 24819–24824.
Yang W, Lo CG, Dispenza T, Cerione RA (2001). The Cdc42 target ACK2 directly interacts with clathrin and influences clathrin assembly. J Biol Chem 276, 17468–17473.
Yokoyama N, Miller WT (2003). Biochemical properties of the Cdc42-associated tyrosine kinase ACK1. Substrate specificity, autophosphorylation, and interaction with Hck. J Biol Chem 278, 47713–47723.
Yoo AS, Bais C, Greenwald I (2004). Crosstalk between the EGFR and LIN-12/Notch pathways in C. elegans vulval development. Science 303, 663–666.
Zhang X, Pickin KA, Bose R, Jura N, Cole PA, Kuriyan J (2007). Inhibition of the EGF receptor by binding of MIG6 to an activating kinase domain interface. Nature 450, 741–744.
Zoncu R, Perera RM, Sebastian R, Nakatsu F, Chen H, Balla T, Ayala G, Toomre D, De Camilli PV (2007). Loss of endocytic clathrin-coated pits upon acute depletion of phosphatidylinositol 4,5-bisphosphate. Proc Natl Acad Sci USA 104, 3793–3798.